Tumour targeting nanoparticles for fluorescence-guided surgery

Inês Santos Pereira Lebre
ines.lebre@tecnico.ulisboa.pt

Instituto Superior Técnico, Lisboa, Portugal

October 2021

Abstract

Cancer is one of deadliest diseases in the world so, to assist surgeons during tumour excision, a fluorescent nanoparticle system with affinity to cancer cells was developed. The system is based in silica nanoparticles, produced by the Stöber method, incorporating a fluorescent NIR emitting cyanine dye. The chosen dye, a called FIGS-IST-Dye1, with silane groups in its structure for anchoring into the silica matrix during synthesis. For targeting the tumours, the NP were surface covered with folate groups, by two different methods. The two-step method found to yield better surface coverage results, measured by ^{1}H NMR.A photo-degradation test showed that the dye inside the particles has a better photo-stability. Cell viability tests with fibroblast showed that the particles obtained are biocompatible at concentrations below 100 μg/mL. The nanoparticles developed in this work have excellent potential for use in fluorescence guided surgery using current NIR surgical equipment.

Keywords: Nanoparticle, Indocyanine Green (ICG), Fluorescence-guided surgery (FGS), Selective targeting, Folic acid

1. Introduction

According to the World Health Organization (WHO), cancer is the second most common cause of death, being responsible for about 10 million deaths per year.[1] It is characterized by an uncontrolled development of cells that lost the ability to function in a normal way, due to damage in the DNA. As the tumour grows the nutrients and oxygen needs increase, and it signals the body to form new blood vessels, in a process called angiogenesis. This also facilitates the spread to other places, through the bloodstream or lymphatic system, creating metastasis. The earlier it is detected and treated, the higher the cure rates.[2]
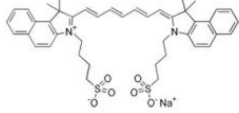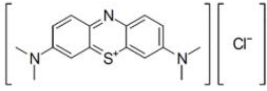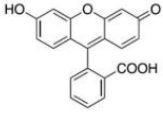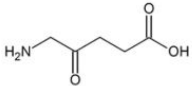
1.1. Fluorescence Guided Surgery

One treatment option is removal surgery, where the goal is to obtain negative margins, meaning that no cancer cells are found by the pathologist when examining the outer edge of the removed tissue. [3] Nevertheless, if a small number of cells remains, they can multiply and lead to recurrence. However, positive margins happens in 50-70% of curative surgeries, so to help surgeons, real-time imaging techniques, like fluorescent probes and optical imaging devices can be used to improve the perception of tumour cells. This technique is called Fluorescence Guided Surgery (FGS). The dye needs to have a high tissue penetration and minimal light scattering. In this case, Near Infrared (NIR) is the best option, being the golden range between 700-900nm, as it meets the needs previously mentioned. [4, 5] Table 1 compiles the dyes already in use in FGS, which are indocyanine green (ICG), methylene blue (MB), fluorescein, and 5-Aminolevulinic acid (5-ALA). They emit in different wavelengths and are applied to different organs and systems. Indocyanine Green is a fluorescent marker and one of the most used in Near Infrared FGS. It was the first to be approved by FDA for *in vivo* use in humans. [6] It is a water-soluble molecule that binds to proteins. While remaining in circulation, allows a lymphatic mapping and liver and biliary evaluation. It is excreted by the hepatic system within 24h, without evidence of toxic effects. [6, 5] Nevertheless, ICG has poor photostability, especially in aqueous environments, and poor hydrolytic stability, which implies time-limited surgeries. It is half live goes up to half an hour. [7]

IRDye800CW is a marker from the cyanine family that is still not US-FDA approved for surgery but is in clinical trials for pancreatic and colorectal cancer.[5] In PBS, the maximum absorbance was 774nm, and emission 789nm. In studies with IRDye800Cw, there were no signs of toxic effects in the animals tested, being the maximum concentration evaluated 20 mg/kg. [8]

Table 1: Structures and properties of fluorescence probes. Reprinted from [6]

FDA approved fluorescence probe	Molecular structure	Excitation wavelength (nm)	Emission wavelength(nm)
Indocyanine green (ICG)		780	820
Methylene blue (MB)		670	690
Fluorescein sodium		494	512
5-Aminolevulinic acid (5-ALA)		380–440	620 (alkaline pH); 634 (acidic pH)

1.2. Tumour Targeting

Targeting allows a dye that is injected or delivered to the body, to accumulate at the desired location and allow its visualization. Selective targeting leads to an adequate biodistribution, minimizing toxicity and, protecting it from the multiple threats in the body and therefore increasing the efficiency and minimizing side effects. [6] Targeting can be passive or active. Passive targeting makes use of the natural body reaction towards a macromolecule, by a phenomenon called enhanced permeability and retention (EPR) effect. This effect is based on the vascularization differences between tumours and healthy tissue. Surrounding a tumour there is an excessive vascularization and higher permeability, while in healthy tissue, the molecules have trouble penetrating the vessels. This effect combined with the lack of lymphatic drainage in a tumour leads to an accumulation of particles. According to some studies, the range of 30-50nm is the optimum for cellular uptake. [9] Active targeting uses specific receptors and endocytosis systems to deliver a particle at the desired site. Folic Acid is an example of this. Folic Acid, fig.1 is a hydrosoluble B vitamin important in the DNA and RNA synthesis and repair as well as protein and haemoglobin formation. It is known that some cancers have the folate receptor over-expressed, due to the high rate of cellular proliferation when compared to healthy tissue. The over expression that can be exploited as an active targeting form using folic acid to bind to the folate receptors leading to receptor-mediated endocytosis. [10, 11]
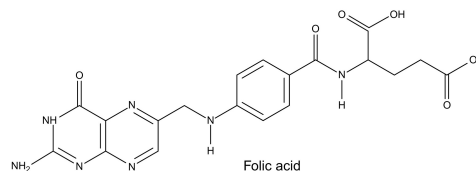

Figure 1: Structure of Folic Acid. [12]

1.3. Silica Nanoparticles

Nanotechnologies are considered to have been introduced by physics Nobel laureate Richard P Feynman in 1959, but the term was invented by Norio Taniguchi, a professor from Tokyo University of Science, in 1974, and are characterized by particles with a diameter under 100nm. [13] The more stable form is spherical. The surface can be modified physically or chemically for example, by adding targeting groups or redefining the surface charge to better fit the pretended goal. [14, 15]

Nanoparticles have gained interest in theranostic (therapeutic and diagnostic) systems. One group with great results in biomedical applications are Silica Nanoparticles (SiNPs), which have been used as carriers and supports in catalysis, drug delivery, imaging, etc. The advantages of SiNPs include the facility to control their diameter and low size dispersion, biocompatibility and lower aggregation compared to polymer-based nanoparticles. [11, 15] One way to produce SiNPs is by the Stöber method, a sol-gel method, developed in 1968 by Werner Stöber, Arthur Fink and Ernst Bohn.[16] This process involves a colloidal solution to get well-defined particles, monodispersed spheres and with uniform composition. The morphology of the particles can

be easily tuned, by simply adjusting reaction parameters (temperature, pH, source of silica...) and can be used in multiple applications such as ceramics, chromatography, catalysis, paints, pharmaceuticals, optical imaging, etc. [16, 17]

1.4. Objectives

During the excision of a tumour, the removal of all cancerous cells is extremely important to minimize the recurrence rates. To help surgeons, fluorescent probes are used to better define the tumour margins. The objective of this thesis is to develop tumour targeting fluorescence nanoparticles for fluorescence-guided surgery. The nanoparticle can both protect the dye and improve its accumulation on tumorous tissue by functionalization with target groups.

For developing the system, a easy to produce perylenediimide derivative was used. Perylenediimides are dyes with a good photochemical and thermal stability, photophysical properties that can be tunned, replacing substituents, in the perylene core positions (Structure represented in fig 2) However, it is not an approved fluorescent probe for FGS. The initially incorporated dye into the Silica Nanoparticles was the bis(propyl)trietoxisilane perylenediimide, usually known as pigment red 179 (Fig.2). [4]
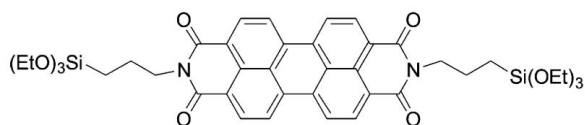

Figure 2: Structure of bis(propyl)triethoxysilane perylenediimide.[18]

To improve tumorous affinity, we used folic acid as an active targeting agent. Since our goal was to functionalize only the external layer, without compromising the structure and size dispersion, the functionalization process chosen was post-grafting, with the carboxylic acid of the folate reacting with the amine-functionalized SiNP. [19, 20]In the two steps route, the particles are activated with APTES, washed and then the folic acid is added to the SiNPs and in the one, a mixture of APTES and Folic Acid is left stirring and then the particles are added. Both methods were tested and characterized with and the most reliable chosen, to begin using the chosen FGS dye, FIGS-IST-Dye1 (fig.3). This compound is an altered form from the IRDye800CW family. Its emission is in the NIR (outside the range of biological autofluorescence), allowing a good differentiation of tumour and healthy tissue. The alkoxide groups present on its structure allows its incorporation inside the silica network during the Stöber process, by a covalent bond with the reactive organosilicates. [21]
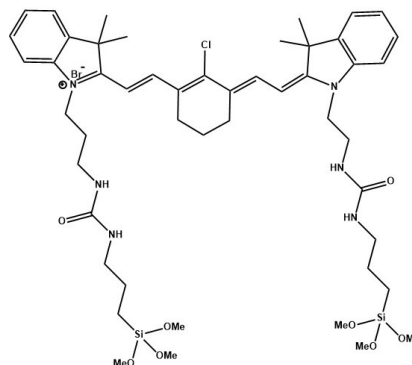

Figure 3: Structure of FIGS-IST-Dye1.

The dye containing SiNPs are biocompatible but since our goal is to use it in Flourescence Guided Surgery (FGS), we need to reassure that there is no toxicity. So we performed a cell viability test to access the biocompatibility of the final system.

2. Experimental Procedure

2.1. Reagents and Solvents

Ammonium hydroxide solution (NH_3 basis, $28.0 - 30.0\%$), Tetraethyl orthosilicate ($TEOS, \geq 99.0\%$), 3-aminopropyl triethoxysilane (APTES, 99%), N,N'-Dicyclohexylcarbodiimide (DCC,99%), Dimethyl Sulfoxide (DMSO, anhydrous, $\geq 99.9\%$) were purchased from Sigma-Aldrich. Ethanol ($\geq 99.8\%$), N,N-Dimethylformamide (DMF, HPLC grade, $\geq 99.9\%$) and s-Trioxane (1,3,5-trioxane,99+%) from Honeywell Fluka, Fisher Scientific. Dicloromethane (DCM, HPLC- Isocratic grade- Stabilized with amylene) from Carlo Erba. Molecular sieves (3A, 2-5mm, Hygroscopic) from Alfa Aesar. Presto-Blue™ (PB) used from Invitrogen by ThermoFisher Scientific, Carlsbad, CA, USA. Dulbecco's Modified Eagle's Medium (DMEM) and Fetal Bovine Serum (FBS) from gibco and penicillin-streptomycin all bought from Thermo Fisher Scientific. L929 cell line purchased from European Collection of Authenticated Cell Cultures.

2.2. Synthesis of Stöber Silica Nanoparticles

The dye in use, PDI and then FIGS-Dye-IST1, (5 to 10 mg) was dissolved in a small quantity of absolute ethanol and ultra-sonicated. The solution was filtered through a 0.2 μm cellulose filter, to remove insoluble clusters, and transferred into a 250 mL polypropylene flask. Ethanol, Mili-Q Water and NH_3 were added (Table 2) after, TEOS was added to the mixture and the temperature increased to 40 ºC and left overnight. The nanoparticles were centrifuged and washed three times with absolute

ethanol (90 000G, 20 min). The particles were dried in an oven at 60 ⁰C overnight. The amount of NP collected was around 500 mg in each synthesis.

Table 2: Reagents quantities used in the different synthesis.

Synthesis	Absolute Ethanol (g)	Mili-Q H_2O (g)	NH_4OH (mL)	TEOS (mL)
Si1	86.656	9.021	1.51	4.46
Si2	64.656	9.021	1.51	4.46
Si3@PDI	86.656	9.928	1.51	4.46
Si4@PDI	86.656	9.526	1.51	4.46
Si5@FIGS	86.656	9.928	1.51	4.46
Si6	866.56	90.21	15.1	44.6

The one litre reaction was performed to evaluate the possibility of scaling up the process. All the reagents quantities were multiplied by 10 times. 50 mL from the initial solution (Si6A) were transferred to a 250 mL PP flask (Si6B) for comparison.

2.3. Surface functionalization of Silica Nanoparticles

To functionalize the SiNPs, two different routes, one and two steps routes, were followed in order to obtain the more reproducible one. The quantities of APTES used was tailored to each experiment, to deliver two molecules per nm^2.

2.3.1 Two Steps Route

The following procedure was performed as described in [19]. Initially, SiNP(0.250 g) were added to 4.5 g of toluene, and ultrasonicated. APTES (0,0191 g) was added and the reaction was left stirring at 120 ⁰C for 48 h. The SiNP were collected and washed with absolute ethanol three times (90 000 G, 20 min).

The second steps starts by degassing with argon a 50mL round bottom flask, FA (0.0148 g) and DCC (0.1370 g). After, dry DMF (3 mL), DMSO (1 mL) and the amino functionalized particles dispersed in DMF were added and the mixture was left stirring overnight at room temperature. The particles were washed with DCM and absolute ethanol three times (90 000 G, 20 min).

2.3.2 One step Route

The following procedure was performed as described in [20]. DMSO (2.0509 g), FA (0.0607 g), DCC (0.0327 g) and APTES (0.0387 g) where mixed in a 50 mL round bottom flask and left stirring, under argon atmosphere, for 6 h at room temperature. After, 126 mg of SiNP were dispersed in 12 mL of toluene and added to the reaction mixture. The reaction was left stirring for 72 h, at room temperature. Thereafter, the NPs were washed three times with absolute ethanol and dried in the oven.

2.4. Cell Viability

The toxicity effect of the NP was evaluated by resazurin based assay using PrestoBlue™ reagent. Briefly, L929 cell line were seeded in 96-well tissue cultured plates at an initial density of $1x10^4$ cells per well and left overnight in CO_2 incubator (5%) at 37 °C. Then, cell medium (DMEM supplemented with 10 % FBS and 1 % penicillin-streptomycin) was discarded and replaced with a solution of different NP doses previously prepared in a complete cell culture medium. L929 cells were incubated for additional 24 h. Finally, the PB viability assay was performed accordingly with PrestoBlue TM reagent kit protocol. The resazurin conversion into resorufin was monitored by measuring fluorescence intensity (excitation 530 nm, emission 590 nm) in a microplate reader (BMG Labtech, Polar Star Optima) at 37 ⁰C. The test were performed by Adriana Bastos Cruz.

3. Results and Discussion

3.1. Synthesis of Silica Nanoparticles

As previously described, the SiNP were synthesized using the Stöber method. Initially, two syntheses (Si1 and Si2) were performed without any modification just to learn the process. In the next particle synthesis, a dye was incorporated into the reaction mixture. In reactions 3 and 4 we incorporated PDI and in reaction 5 FIGS-IST-Dye1. The quantities were presented in table 2.

After each synthesis, the diameteres of the particles were measured using Dynamic Light Scattering (DLS) and TEM. The diameters were obtained at room temperature and the results are shown in Table 3. DLS values by number were obtained from the average of 5 measurements and the TEM diameters were obtained from 70 particles, using image software ImageJ.

Table 3: Diameter of the SiNP measured by DLS and TEM.

Particles	DLS Average diameter (nm)	TEM Average diameter (nm)
Si1	40 ± 3	39 ± 3
Si2	80 ± 3	80 ± 3
Si3@PDI	24 ± 1	24 ± 3
Si4@PDI	32 ± 1	32 ± 3
Si5@FIGS	37 ± 2	33 ± 3
Si6A	65 ± 2	65 ± 5
Si6B	66 ± 3	69 ± 7

Looking at 2 and 3, we can confirm that when increasing the water quantities, consequently smaller concentrations of ammonium hydroxide and lower pH, leads to smaller particles due to a decreased rate in the condensation phase. [21]

TEM measurements are similar to the number average diameter obtained by DLS. [22] From the

correlograms and diameters standard deviation (the higher value is 12,5%), we can ensure that all the particles were fully dispersed and with uniform sizes. [23]

TEM imaging allows direct visualization of the particles and confirms if their morphology and dimensions are under the target values (the optimal range for particle uptake is 30-50nm). [9] In fig.4, SiNP reveal spherical morphology and uniform size distribution, as previously expected (Table.3). Some aggregation is present that can be justified by sample preparation protocol.

After centrifuging Si5@FIGS, a pink solution was obtained, instead of the normal transparent or greenish, like the dye (fig.5). After the first centrifugation, all the other washes solutions were transparent. From the TEM images, no structural differences appears to be present, so more tests need to be performed to clarify the cause of such colour.

In fig.6, we can see the particles synthesized in large quantities (Si6A). Some solution was transferred to a smaller flask (Si6B) giving us room for comparison. We can confirm that both solutions reached a spherical and uniform morphology, having the smaller solution (Si6B) resulting in slightly bigger particles. This difference can be a result of differences in the reaction stirring in each flask. The quantities used for this reaction were the same used in the first test synthesis (Si1) but resulted in bigger particles, which can be easily explained by the absence of temperature. Si1 was performed at 40 ºC while Si6A and B were at room temperature. Higher temperatures lead to higher hydrolysis rates and therefore an outburst of nucleation points that creates smaller particles. [17]

3.2. Silica NP Functionalization

To promote the selective targeting of cancer cells, the particles were externally modified with Folic Acid (FA). To evaluate the incorporation, two procedures were tested. After functionalization, the Zeta potentials were measured to, confirm the modification. When functionalizing there is a substitution of the alcohol groups by amines. Since alcohols are more negatively charged, when replacing them we can see an increase in the zeta potential value. The results are presented in Table 4.

Table 4: Zeta Potential in multiple functionalizations.

Reaction	Original (mV)	Two Steps (mV)	One Step (mV)
Si3@PDI	(-36.1 ± 0.4)	(-24.9 ± 0.5)	(-1.4 ± 0.3)
Si5@FIGS	(-27.2 ± 0.1)	(-3.1 ± 0.7)	-

The one step functionalization process was not reproduced in the Si5@FIGS nanoparticles for lack of reliability as we will explain further ahead.

To quantify the amount of folic acid incorporated we used Nuclear Magnetic Resonance (NMR), using trioxane as the reference, deuterium oxide as solvent and NaOH to dissolve the silica network. For comparison purposes, a spectrum of non functionalized particles were obtained (Fig 7). We can identify at 4.79ppm the D_2O peak that works as a reference to correct spectrum shifts. At 5.18 ppm we have trioxane and, at 3.55 and 1.07 ppm we observe the ethoxy groups (respectively from the CH_2 and CH_3), corresponding to residual ethanol from washing the particles, that remains entrapped in the matrix even after drying. [24]
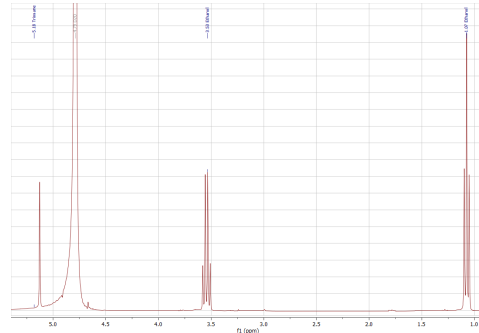

Figure 7: ^1H NMR of non functionalized Si3.

This method allows the quantification of each functional group added to the SiNPs, due to the presence of trioxane. The reference is added in a known concentration so that we can use its peak to extrapolate the concentration of the other molecules. In spectra 8 of Si3 functionalized by the 2-step method, we see the peak assignment for the carbon chain and amine left from APTES, and for the folic acid. The other obtained spectrum are presented in appendix. In Table 5, we have the obtained results for peak integration.

Table 5: Quantification of SiNPs functional groups (mM of APTES/Folic acid by gram of SiNP, molecules per nm^2 of SiNP surface and molecules per SiNP).

Reaction		mMol/g	molecules/nm^2	molecules/particle
Two Step (Si3)	APTES	0.41	1.56	2830
	Folic Acid	0.15	0.59	1067
One Step (Si3)	APTES	2.9	11.26	20379
	Folic Acid	0.77	2.99	5420
One Step (Si4)	APTES	2.18	11.19	35992
	Folic Acid	1.32	6.80	21872
Two Step (Si5)	APTES	0.55	2.89	9902
	Folic Acid	0.12	0.64	2182

When functionalizing the SiNPs, the amount of APTES used was calculated to have a surface coverage of 2 molecules/nm^2 to ensure a good functionalization without overlapping of APTES in one area. Some variations are expected, so the values obtained by the Two step method are reliable.
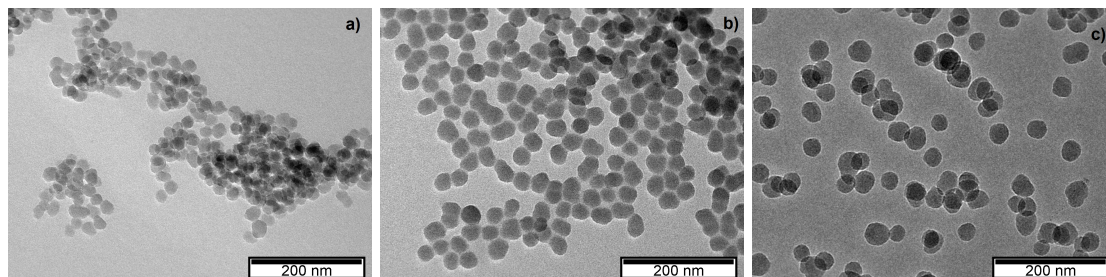
Figure 4: TEM images from reactions: Si3@PDI (a), Si4@PDI (b), Si5@FIGS (c).
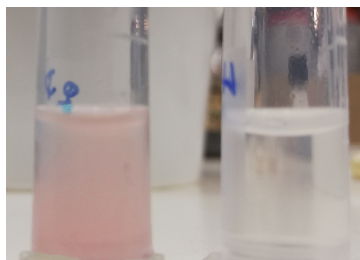

Figure 5: Reactional mixture of Si5@FIGS after first wash (left) and second (right).
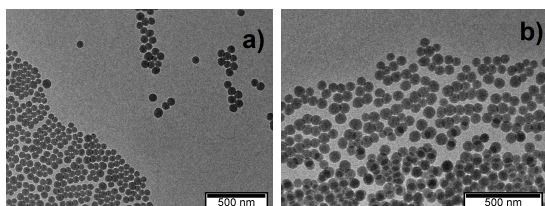

Figure 6: TEM images from reaction: Si6A (a), Si6B (b).

The smaller quantities of Folic Acid when compared with APTES are explained by the larger size of the folic acid molecule (occupies more volume). When we look at the values obtained in Si3 by one step procedure, we can presume to be wrong because it is not physically possible. The same procedure was repeated for Si4, to ensure if it wasn't an experimental error, and once again given values highly contestable. These high values can be a result of folic acid condensation, leaving aggregates. Therefore, when recreating the procedure with FIGS-IST-Dye1, we only used the method with feasible results, the 2-step method.

4. Fluorescence Studies

The main goal of the work is to allow a better identification of tumour tissue during fluorescence-guided surgery. So we have to ensure that the fluorescence properties of the dyes are preserved during synthesis. The fluorescence spectrum of PDI, in toluene without any modifications peaks at 537, 559 and 628 nm [25]. After incorporating in the silica matrix and functionalization, we obtained the following spectra (fig.9). As we can see, the spectrum of the particles is similar to the specific of the free dye. The integrity of the dye was not compromised and the presence of the folate groups does not interfere with the fluorescence. The spectra presents a mirror image and a small stokes shift between emission and excitation.

The same study was performed for the Si5@FIGS particles (Fig.10). The spectra presents a shift from the free dye to the particle caused by the use of different solvents in each measurement (methanol to water). In this range, we can see there were no changes in the fluorescence of the dye when incorporated into a nanoparticle. But if the excitation is further away from the main peak (790 nm), we can see a new peak, at 613 nm, that was not expected (fig.11). That new peak can be associated with the presence of colour in the reaction mixture after centrifuging. A spectra of the reaction mixture was taken (fig.12), showing that the component left has the same emission wavelength has the new peak at Si5@FIGS. A possible explanation is that some of the dye was degraded due to the synthesis pH.
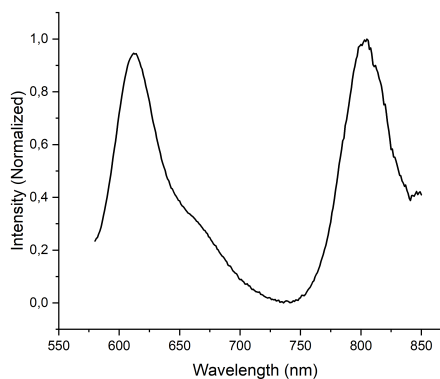

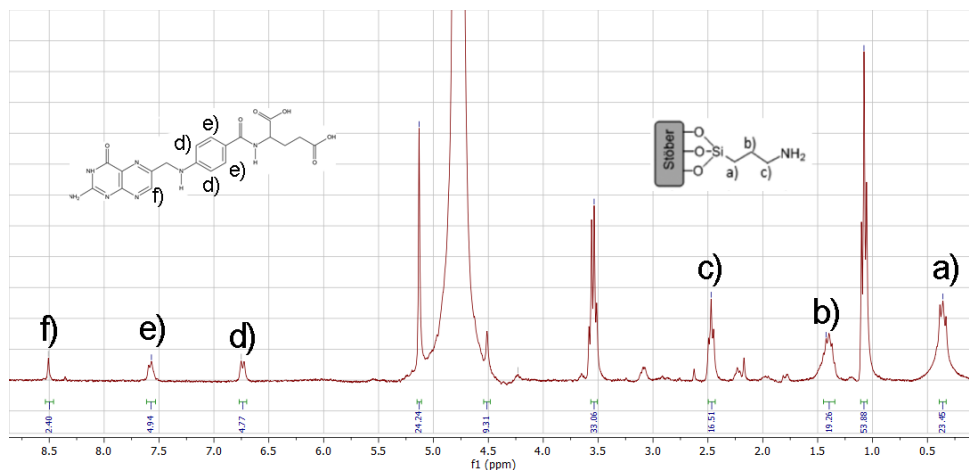Figure 11: Emission spectrum of Si5@FIGS with excitation at 550 nm.

Figure 8: ^1H NMR of Si3-PDI functionalized by the Two Step method, with peaks assignment.
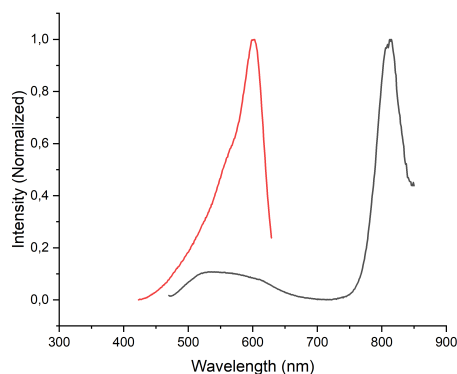

Figure 12: Spectra of the solution obtained after centrifuging the reaction mixture obtained. In red, we have excitation curves (em= 650 nm) and at black emission (ex= 450 nm).
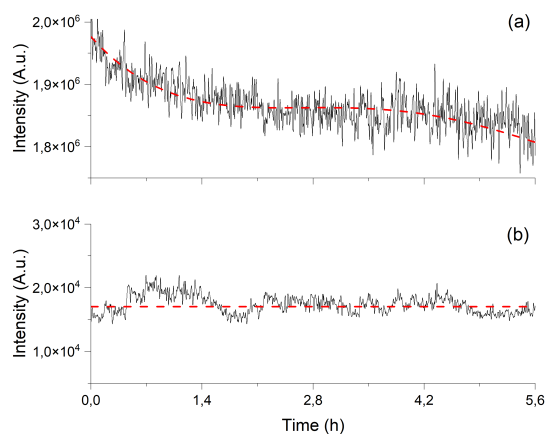

Figure 13: Fluorescence intensity at 800 nm with 680 nm excitation for free dye (a) and Si5@FIGS (b) for 5.6h. Red lines are a guide to the eye.

5. Stability test

Excision surgeries are long and can take hours. So when using fluorescence-guided surgery, the dye will be irradiated for a long time and it cannot degrade and lose fluorescence properties. To prove our model, we performed a time-based measurement of fluorescence with the free dye and Si5@FIGS. The fluorescence intensity was recorded at 800 nm for 5.6 hours as a proof of concept for the better stability of the dye inside a particle, fig.13. The intensity values are not relevant since the values are proportional to concentration, and we the incorporation of dye inside the particles were not measured so we cannot know the concentration of fluorescence molecules inside the particles for comparison. [26]

As we can see, there is a 17 % reduction of the free dye fluorescence intensity during the 5.6 h irradiation. In the particles, almost no reduction is observed. This validates the photo-degradation protection from the silica matrix, due to the oxygen shielding effect. The presence of oxygen promotes the development of free radicals, mostly in the presence of UV or visible light. That interferes with the structure, attacking especially the double covalent bonds and aromatic moieties, leading to a loss of fluorescence. [27] We demonstrated that for at least 5.6 h we can have the nanoparticles irradiated without a significant loss of fluorescence intensity, being a great indicator for use in FGS.

6. Cell Viability

If the nanoparticles are going to be used in Flourescence Guided Surgery (FGS) they cannot be toxic to human cells. To evaluate their toxicity, a cell viability test was performed. This determines the per-
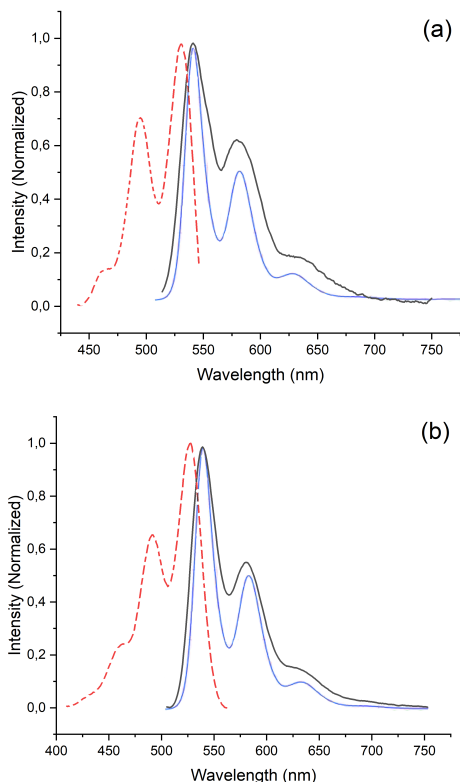
Figure 10: Normalized fluorescence spectrum of Si5@FiGS (red) in H_2O and free FIGS-IST-Dye1 (black) in methanol. Excitation (dashed curves) of the NP measured at 840 nm, and of the free dye at 825 nm. Emission (solid curve) of the NP measured at 680nm, and of the free dye at 710 nm.

Figure 9: Normalized fluorescence spectrum of (a) Si3@PDI, functionalized via One Step method in H_2O and (b) Si4@PDI functionalized via Two Step method in H_2O. In dashed red, we have excitation curves (em= 580 nm) and at solid black, emission curves (ex= 490 nm). In blue we have the spectra of PDI before synthesis, in toluene.

centage of viable cells comparing to control (CTR, cells incubated with complete medium). The concentrations were measures sequentially from 1.5 to 200 μg of particles per mL of water in a cell plate (fig.14).
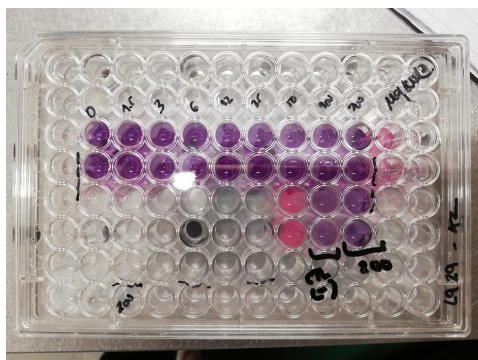

Figure 14: 96-Well Cell Culture Plate.

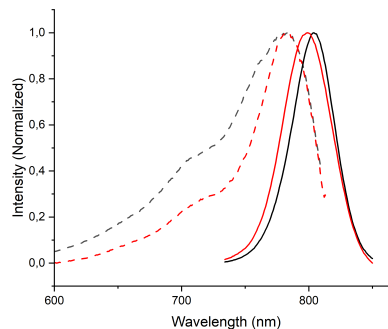The colour changes from purple-blue to red and these changes can be measured using fluorescence

or absorbance measurements. [28] The pinker the colour and therefore higher counts, the more cells are viable and reducing the solution. In Table 6, the results were measured one hour after the introduction of the particles and PrestoBlue™. In Table 7, the particles were added to the cells, and incubation was procced for 48 h. PrestoBlue™ was then added, and the results measured one hour later.

Due to experimental errors, we have values higher than 100 %, that are easily explained by small differences in the number of cells added, and/or small variations in the volume of PrestoBlue™ added to each well. In the concentration of 200 μg/mL, some precipitation was noticed, so it is clear to assume that this concentration was too high to be further used. Now looking at the cell viability, we can see that 100 and 200 μg/mL present some degree of toxicity to the cells, being the last one very significant. For the other values, we can say that the particles are biocompatible.

7. Conclusions

In this work, silica nanoparticles were synthesize with an incorporated dye and functionalized with folic acid for better targeting. The synthesis itself presented no challenges being the sizes easily tailorable and resulting in monodispersed spherical particles.

The incorporation of the dye was proved by the fluorescence spectra, nevertheless the presence of unexpected peaks lead us to think that some degradation happened and a by product was included in the matrix, since it remained in the particles even after washing. This sub-product is thought to be one of the constituent groups of the FIGS-IST-Dye1 obtained through degradation due to pH, but needs further investigation to elucidate the origin.

Table 6: Cell viability after 1 h of PrestoBlue™ introduction.

(μg/mL)	0	1.5	3	6	12.5	25	50	100	200
Counts	23535	-	20882	20065	23143	20446	17950	19453	10647
Cell Viability (%)	100	-	88	84	98	86	74	82	42

Table 7: Cell viability after 48 h incubation.

(μg/mL)	0	1.5	3	6	12.5	25	50	100	200
Counts	8224	8760	11379	12835	13553	12690	12660	7171	6666
Cell Viability (%)	100	108	146	168	178	166	165	85	77

For the functionalization with folic acid, two processes were tested and quantified through NMR. The one step method resulted in unrealistic surface coverage values. The two step was then chosen for further syntheses, seeing that the surface coverage obtained is consisted with the quantification selected. The folic acid remained intact during the functionalization process and was successfully connected to the particles.

As a proof of concept for the particle oxygen shielding effect, a kinetics fluorescence study was performed. The particles and the free FIGS-IST-Dye1 were irradiated at 680 nm for 5.6 h, and the emission measured at the 800nm. Over time,it was verified that the dye on its own had a reduction of intensity more significant than inside the particle. That reduction is associated with the photodegradation of the structure, so the SiNP were proven to protect FIGS-IST-Dye1.

Finally, to ensure the biocompatibility, a cell viability test was performed. In general, the particles present no toxicity to the cells. At concentrations superior to 100 μg/mL that is no longer true. At 200 μg/mL, we can also verify some precipitation in the well.

In conclusion, the goal of the thesis was successfully achieved. We were able to produce functional nanoparticles that are fluorescence under NIR light and with targeting groups for cancer cells. Further tests need to be done, first to confirm what was the sub product obtained during the synthesis of SiNP with FIGS-IST-Dye1 and second, to prove the higher affinity and accumulation of the nanoparticles in the tumorous tissue.

References

[1] "Cancer Fact Sheet," Available at https://www.who.int/news-room/fact-sheets/detail/cancer [Accessed on 04/04/2021].

[2] "How cancer strats, grows and spreads-Canadian Cancer Society," Available at https://www.cancer.ca/en/cancer-information/cancer-101/what-is-cancer/how-cancer-starts-grows-and-spreads/?region=on [Accessed on 24/05/2021].

[3] "Definition of margin - NCI Dictionary of Cancer Terms - National Cancer Institute," Available at https://www.cancer.gov/publications/dictionaries/cancer-terms/def/margin [Accessed on 28/10/2021].

[4] T. Ribeiro, S. Raja, A. S. Rodrigues, F. Fernandes, C. Baleizão, and J. P. S. Farinha, "NIR and visible perylenediimide-silica nanoparticles for laser scanning bioimaging," *Dyes and Pigments*, pp. 227–234, 2014.

[5] T. Nagaya, Y. A. Nakamura, P. L. Choyke, and H. Kobayashi, "Fluorescence-guided surgery," *Frontiers in Oncology*, p. 314, 2017.

[6] Y. Zheng, H. Yang, H. Wang, K. Kang, W. Zhang, G. Ma, and S. Du, "Fluorescence-guided surgery in cancer treatment: current status and future perspectives," *Annals of Translational Medicine*, pp. S6–S6, 2019.

[7] T. Mangeolle, I. Yakavets, S. Marchal, M. Debayle, T. Pons, L. Bezdetnaya, and F. Marchal, "Fluorescent nanoparticles for the guided surgery of ovarian peritoneal carcinomatosis," *Nanomaterials*, pp. 1–20, 2018.

[8] M. V. Marshall, D. Draney, E. M. Sevick-Muraca, and D. M. Olive, "Single-Dose Intravenous Toxicity Study of IRDye 800CW in Sprague-Dawley Rats," *Molecular Imaging and Biology*, pp. 583–594, 2010.

[9] P. Foroozandeh and A. A. Aziz, "Insight into Cellular Uptake and Intracellular Trafficking of Nanoparticles," *Nanoscale Research Letters*, 2018. [Online]. Available: /pmc/articles/PMC6202307//pmc/articles/

PMC6202307/?report=abstracthttps://www.ncbi.nlm.nih.gov/pmc/articles/PMC6202307/

[10] T. Shukla, N. Upmanyu, S. P. Pandey, and M. S. Sudheesh, *Chapter 14 - Site-specific drug delivery, targeting, and gene therapy*, A. M. Grumezescu, Ed. William Andrew Publishing, 2019.

[11] G. L. Zwicke, G. A. Mansoori, and C. J. Jeffery, "Utilizing the folate receptor for active targeting of cancer nanotherapeutics," *Nano Reviews*, p. 18496, 2012.

[12] M. Bansal, N. Singh, S. Pal, I. Dev, and K. M. Ansari, "Chemopreventive Role of Dietary Phytochemicals in Colorectal Cancer," *Advances in Molecular Toxicology*, pp. 69–121, 2018.

[13] M. Benelmekki, "An introduction to nanoparticles and nanotechnology," *Designing Hybrid Nanoparticles*, pp. 1–14, 2015.

[14] A. M. Santiago, "Biocompatible Hybrid Materials for Fluorescence Imaging Biodiagnostic Applications Biological Enginnering Examination Committee," Ph.D. dissertation, IST, 2013.

[15] A. M. Santiago, T. Ribeiro, A. S. Rodrigues, B. Ribeiro, R. F. Frade, C. Baleizão, and J. P. S. Farinha, "Multifunctional Hybrid Silica Nanoparticles with a Fluorescent Core and Active Targeting Shell for Fluorescence Imaging Biodiagnostic Applications," *European Journal of Inorganic Chemistry*, pp. 4579–4587, 2015.

[16] W. Stöber, A. Fink, and E. Bohn, "Controlled growth of monodisperse silica spheres in the micron size range," *Journal of Colloid and Interface Science*, pp. 62–69, 1968.

[17] P. P. Ghimire and M. Jaroniec, "Renaissance of Stöber method for synthesis of colloidal particles: New developments and opportunities," *Journal of Colloid and Interface Science*, pp. 838–865, 2021.

[18] Y. Luo and J. Lin, "Solvent induced different morphologies of bis(propyl)triethoxysilane substituted perylenediimide and their optical properties," *Journal of Colloid and Interface Science*, pp. 625–630, 2006.

[19] M. Cabañas, D. Lozano, A. Torres-Pardo, C. Sobrino, J. González-Calbet, D. Arcos, and M. Vallet-Regí, "Features of aminopropyl modified mesoporous silica nanoparticles. Implications on the active targeting capability," *Materials Chemistry and Physics*, pp. 260–269, 2018.

[20] E. Ortiz-Islas, A. Sosa-Arróniz, M. E. Manríquez-Ramírez, C. E. Rodríguez-Pérez, F. Tzompantzi, and J. M. Padilla, "Mesoporous silica nanoparticles functionalized with folic acid for targeted release Cis-Pt to glioblastoma cells," *Reviews on Advanced Materials Science*, pp. 25–37, 2021.

[21] J. F. Bringley, T. L. Penner, R. Wang, J. F. Harder, W. J. Harrison, and L. Buonemani, "Silica nanoparticles encapsulating near-infrared emissive cyanine dyes," *Journal of Colloid and Interface Science*, pp. 132–139, 2008.

[22] "Intensity - Volume - Number | Technical Notes Malvern Panalytical," Available at https://www.malvernpanalytical.com/en/learn/knowledge-center/technical-notes/TN101104IntensityVolumeNumber.html?utm_source=MaterialsTalks&utm_medium=blog&utm_campaign=null&utm_term=9612&utm_content=entryContentLink [Accessed on 18/10/2021].

[23] "Dynamic Light Scattering (DLS) | Common Terms Defined | Malvern Panalytical," Available at https://www.malvernpanalytical.com/en/learn/knowledge-center/whitepapers/WP111214DLSTermsDefined [Accessed on 18/10/2021].

[24] C. I. C. Crucho, C. Baleizão, and J. P. S. Farinha, "Functional Group Coverage and Conversion Quantification in Nanostructured Silica by 1 H NMR," *Analytical Chemistry*, pp. 681–687, 2017. [Online]. Available: https://pubs.acs.org/doi/10.1021/acs.analchem.6b03117

[25] "Perylene-diimide, [PDI]," Available at https://omlc.org/spectra/PhotochemCAD/html/143.html [Accessed on 26/10/2021].

[26] H. Itagaki, "Fluorescence Spectroscopy," in *Experimental Methods in Polymer Science: Modern Methods in Polymer Research and Technology*. Academic Press, 2000, pp. 155–260.

[27] B. R. Hammond, B. A. Johnson, and E. R. George, "Oxidative photodegradation of ocular tissues: Beneficial effects of filtering and exogenous antioxidants," *Experimental Eye Research*, pp. 135–150, 2014.

[28] "PrestoBlue™ Cell Viability Reagent," Available at https://www.thermofisher.com/order/catalog/product/A13261 [Accessed on 30/10/2021].